# Modelling Turbulent Combustion Coupled with Conjugate Heat Transfer in OpenFOAM


**Mohamed el Abbassi, Domenico Lahaye, and Kees Vuik**

**Abstract** This paper verifies a mathematical model that is developed for the open source CFD-toolbox OpenFOAM, which couples turbulent combustion with conjugate heat transfer. This feature already exists in well-known commercial codes. It permits the prediction of the flame's characteristics, its emissions, and the consequent heat transfer between fluids and solids via radiation, convection, and conduction. The verification is based on a simplified 2D axisymmetric cylindrical reactor. In the first step, the combustion part of the solver is compared against experimental data for an open turbulent flame. This shows good agreement when using the full GRI 3.0 reaction mechanism. Afterwards, the flame is confined by a cylindrical wall and simultaneously conjugate heat transfer is activated and analysed. It is shown that the combustion and conjugate heat transfer are successfully coupled.

## 1 Introduction

Industrial furnaces such as kilns are pyroprocessing devices in which a heat source is generated via fuel combustion. In order to make a numerical prediction of the temperature distribution along a solid (e.g. the material bed, furnace walls, or heat exchanger), one must model the coupled effects of the occurring physical phenomena. The heat released by the turbulent flame may be transferred to the solid through all heat transfer modes: thermal radiation, conduction, and convection. Thermal radiation is transmitted to the solid directly from the flame, or indirectly from the hot exhaust and other solids. Conduction occurs within solids and through contact with other solid particles, while convective heat may be exchanged via any contact between gas and solids. In return, the fluctuating heat transfer affects the turbulent flow and flame characteristics. Controlling the flame enables achieving

M. el Abbassi · D. Lahaye · K. Vuik (✉)
Delft Institute of Applied Mathematics, Delft University of Technology, Delft, The Netherlands
e-mail: M.elAbbassi@tudelft.nl; D.J.P.Lahaye@tudelft.nl; C.Vuik@tudelft.nl



F. J. Vermolen, C. Vuik (eds.), *Numerical Mathematics and Advanced Applications ENUMATH 2019*, Lecture Notes in Computational Science and Engineering 139, https://doi.org/10.1007/978-3-030-55874-1_113

the desired heat distribution with minimum emissions. Coupling combustion and heat transfer is essential to find optimal solutions to these conflicting interests, particularly in view of increasing environmental concerns (which view reducing the furnace emissions and fuel consumption as urgent), along with the growing demand for an increase in furnace production rate.

Incorporating the heat transfer between fluids and solids into one mathematical problem may be referred as conjugate heat transfer (CHT). CHT is implemented in many popular CFD codes. Before this project, there were no publications on coupling turbulent combustion and CHT with the open source CFD-toolbox OpenFOAM. OpenFOAM sets a structured object-oriented framework and includes numerous applications to solve different kinds of CFD-related problems.

An implementation was recently proposed and developed for OpenFOAM by Tonkomo LLC [1, 2], that combines the turbulent-non-premixed-combustion solver reactingFoam with the CHT-solver chtMultiRegionFoam. This provides new opportunities for modelling furnaces or any other combustion and heat transfer related problem. In our work, the capabilities of the new solver are investigated by testing it on the 2D axisymmetric case of the open turbulent flame from the Sandia laboratory, by means of RANS simulation.

Our presented work is structured as follows. First the governing equations of the problem are highlighted. We describe the physical models of OpenFOAM that are needed to solve them and how the regions are coupled for energy transport. Afterwards, the cases and their boundary conditions are presented, followed by a discussion of the results.

## 2 Governing Equations and Numerical Models

In the fluid domain, the Favre-averaged transport equations of mass, momentum, sensible enthalpy and chemical species [3] are respectively described by

$$\frac{\partial(\bar{\rho})}{\partial t} + \nabla \cdot (\bar{\rho}\widetilde{u}) = 0, \tag{1}$$

$$\frac{\partial(\bar{\rho}\widetilde{u})}{\partial t} + \nabla \cdot (\bar{\rho}\widetilde{u}\widetilde{u}) = -\nabla \bar{p} + \nabla \cdot \mu \nabla \widetilde{u} - \nabla \cdot \bar{\rho}\widetilde{u''u''}, \tag{2}$$

$$\frac{\partial(\bar{\rho}\widetilde{Y_\alpha})}{\partial t} + \nabla \cdot (\bar{\rho}\widetilde{u}\widetilde{Y_\alpha}) = \nabla \cdot \bar{\rho}\Gamma \nabla \widetilde{Y_\alpha} - \nabla \cdot \bar{\rho}\widetilde{Y_\alpha''u''} + \widetilde{R}_\alpha, \tag{3}$$

$$\frac{\partial(\bar{\rho}\widetilde{h})}{\partial t} + \nabla \cdot (\bar{\rho}\widetilde{u}\widetilde{h}) = \frac{D}{Dt}\bar{p} + \nabla \cdot \frac{\lambda}{c_p}\nabla \widetilde{h} - \nabla \cdot \bar{\rho}\widetilde{h''u''} + \widetilde{Q}_c + \widetilde{Q}_r, \tag{4}$$

where $\rho$ is the density, $u$ the velocity, $p$ the pressure, $\mu$ the laminar dynamic viscosity, $Y_\alpha$ the species mass fraction of species $\alpha$, $\Gamma$ the species diffusion coefficient, $R$ the reaction rate of species $\alpha$, $h$ the specific sensible enthalpy, $\lambda$ the

thermal conductivity and $c_p$ the specific heat capacity at constant pressure. The heat source terms $Q_c$ and $Q_r$ are due to combustion and thermal radiation, respectively. The over-bar and tilde notations stand for the average values, while the double quotation marks denote the fluctuating components due to turbulence. Note that several source terms (such as body forces and viscous heating) are neglected.

For solid regions, only the energy transfer needs to be solved and therefore the equation of enthalpy for solids, which is the following heat equation, has to be added to the list of transport Eqs. (1)–(4):

$$\frac{\partial(\bar{\rho}h)}{\partial t} = \nabla \cdot (\lambda \nabla T). \tag{5}$$

To couple the thermal energy transport between the fluid and solid domains, two important conditions are required at the interface of the domains to ensure continuity of both the temperature and heat flux:

$$T_{f,int} = T_{s,int} \tag{6}$$

and

$$\lambda_f \frac{\partial T_f}{\partial y}\bigg|_{int,y=+0} = \lambda_s \frac{\partial T_s}{\partial y}\bigg|_{int,y=-0}, \tag{7}$$

where the subscripts $f$, $s$ and $int$ respectively stand for fluid, solid and interface. $y$ is the local coordinate normal to the solid. Unclosed terms appear in the transport equations of the fluid domain due to Favre averaging. These will be treated in this section, followed by the elaboration of the heat transfer at the interface.

## 2.1 Turbulence

The unknown Reynolds stresses (last term of Eq. (2)) are solved by employing the Boussinesq hypothesis that is based on the assumption that in turbulent flows, the relation between the Reynolds stress and viscosity is similar to that of the stress tensor in laminar flows, but with increased (turbulent) viscosity:

$$-\nabla \cdot \bar{\rho}\widetilde{u_i"u_j"} = \mu_t \left( \frac{\partial u_i}{\partial x_j} + \frac{\partial u_j}{\partial x_i} \right) - \frac{2}{3} \left( \rho k + \mu_t \frac{\partial u_k}{\partial x_k} \right) \delta_{ij}, \tag{8}$$

where $\mu_t$ is the turbulent viscosity and $k$ the turbulent kinetic energy. The Reynolds stresses are closed with the Realizable $k$-$\epsilon$ turbulence model, which is widely known for its superior capability over the Standard and RNG $k$-$\epsilon$ models in predicting the mean of the more complex flow features. The model solves two additional transport equations: one for the turbulent kinetic energy $k$, and the other for its dissipation

rate $\epsilon$

$$\frac{\partial(\bar{\rho}k)}{\partial t} + \nabla \cdot (\bar{\rho}\widetilde{u}k) = \nabla \cdot \left[\left(\mu + \frac{\mu_t}{\theta_k}\right)\nabla k\right] + \mu_t \left(\frac{\partial u_i}{\partial x_j}\right)^2 - \bar{\rho}\epsilon, \tag{9}$$

$$\frac{\partial(\bar{\rho}\epsilon)}{\partial t} + \nabla \cdot (\bar{\rho}\widetilde{u}\epsilon) = \nabla \cdot \left[\left(\mu + \frac{\mu_t}{\theta_\epsilon}\right)\nabla \epsilon\right] + \bar{\rho}c_1 S\epsilon - \bar{\rho}c_2 \frac{\epsilon^2}{k + \sqrt{\nu\epsilon}}, \tag{10}$$

where $\theta_k$,$\theta_\epsilon$ and $c_2$ are constants. $S$ is the modulus of the mean strain rate tensor, defined as $S = \sqrt{2S_{ij}S_{ij}}$ and $c_1$ is a function of $k$, $\epsilon$ and $S$. Again, note that the effect of buoyancy and other source terms are neglected. With $k$ and $\epsilon$, the turbulent viscosity can be determined by the following relation:

$$\mu_t = \bar{\rho}c_\mu \frac{k^2}{\epsilon}, \tag{11}$$

where in the Realizable $k$-$\epsilon$ model, $c_\mu$ is a function of $k$, $\epsilon$, the mean strain rate and the mean rotation rate. This is one of the major differences compared to the other $k$-$\epsilon$ models where $c_\mu$ is a constant.

The turbulent scalar fluxes $\bar{\rho}\widetilde{\phi"u"}$ for the scalar chemical species and scalar sensible enthalpy (both denoted as $\phi$) are closed with the Gradient diffusion assumption

$$-\bar{\rho}\widetilde{\phi"u"} = \nabla \cdot (\Gamma_t \widetilde{\phi}), \tag{12}$$

where $\Gamma_t$ is the turbulent diffusivity determined by (assuming Lewis number = 1) the turbulent viscosity $\mu_t$ and turbulent Prandtl number $Pr_t$:

$$\Gamma_t = \frac{\mu_t}{Pr_t}. \tag{13}$$

## 2.2 Combustion

The mean chemical source term $\widetilde{R}_\alpha$ is closed with the Partially Stirred Reactor (PaSR) model. The model developed at Chalmers university allows for the detailed Arrhenius chemical kinetics to be incorporated in turbulent reacting flows. It assumes that each cell is divided into a non-reacting part and a reaction zone that is treated as a perfectly stirred reactor. The fraction is proportional to the ratio of the chemical reaction time $t_c$ to the total conversion time $t_c + t_{mix}$:

$$\gamma = \frac{t_c}{t_c + t_{mix}}. \tag{14}$$

The turbulence mixing time $t_{mix}$ characterizes the exchange process between the reacting and non-reacting mixture, and is determined via the $k$-$\epsilon$ model as

$$t_{mix} = c_{mix}\sqrt{\frac{\mu_{eff}}{\bar{\rho}\epsilon}}, \tag{15}$$

where $c_{mix}$ is a constant and $\mu_{eff}$ is the sum of the laminar and turbulent viscosity. Then the mean source term is calculated as $\widetilde{R}_\alpha = \gamma R_\alpha$, where $R_\alpha$ is the laminar reaction rate of species $\alpha$ and is computed as the sum of the Arrhenius reaction rates over the $N_R$ reactions that the species participate in:

$$R_\alpha = \sum_{r=1}^{N_R} \hat{R}_{\alpha,r}, \tag{16}$$

where $\hat{R}_{\alpha,r}$ is the Arrhenius rate of creation/destruction of species $\alpha$ in reaction $r$. For a reversible reaction, the Arrhenius rate is given by

$$\hat{R}_{\alpha,r} = \psi_{f,r}\prod_{r=1}^{N_R}[C_{\beta,r}]^{\eta'_{\ell,r}} - \psi_{b,r}\prod_{r=1}^{N_R}[C_{\beta,r}]^{\eta''_{m,r}}, \tag{17}$$

where $C_{\beta,r}$ is the concentration of species $\beta$ in reaction $r$, $\eta'_{\ell,r}$ is the rate exponent for reactant $\ell$ in reaction $r$, $\eta''_{m,r}$ is the stoichiometric coefficient for product $m$ in reaction $r$, and $\psi_{f,r}$ and $\psi_{b,r}$ are respectively the forward and backward rate constants given by the Arrhenius expressions.

The chemical time scale can be determined with the following relation:

$$\frac{1}{t_c} = max\left(\frac{-\partial R_\alpha}{\partial Y_\alpha}\frac{1}{\bar{\rho}}\right). \tag{18}$$

## 2.3 Energy

The thermal conductivity $\lambda$ in the averaged transport of the specific sensible enthalpy (Eq. (4)) is replaced by the effective conductivity $\lambda_{eff}$, which incorporates the unknown turbulent scalar flux. From Eqs. (12) and (13), $\lambda_{eff}$ is defined by the Standard and Realizable $k$-$\epsilon$ models as

$$\lambda_{eff} = \frac{\mu}{Pr} + \frac{\mu_t}{Pr_t}, \tag{19}$$

where the turbulent Prandtl number, from experimental data, has an average value of 0.85. The heat release due to combustion $\widetilde{Q_c}$ follows from the calculations of $\widetilde{R_\alpha}$

$$\widetilde{Q_c} = -\sum_{\alpha=1}^{N} \Delta h^o_{f,\alpha} \widetilde{R_\alpha}, \tag{20}$$

where $\Delta h^o_{f,\alpha}$ is the formation enthalpy of species $\alpha$, and $N$ is the total number of species.

## 2.4 Thermal Radiation

To obtain the mean radiation source term $\widetilde{Q_r}$ for the enthalpy transport equation, we employ the P1 approximation in accordance with the previous work, which solves the following partial differential equation for a non-scattering medium

$$-\nabla \cdot \left( \frac{1}{3\kappa} \nabla G \right) = \kappa (4\sigma T^4 - G), \tag{21}$$

where the radiation source term appears on the LHS of the equation. $G$ is the total incident radiation, $\kappa$ is the absorption coefficient of the medium and $\sigma$ is the Stefan–Boltzmann constant. The P1 approximation is subject to the following boundary condition of the third kind

$$-\frac{1}{3\kappa} \mathbf{n} \cdot \nabla G = -\frac{\kappa_w}{2(2-\kappa_w)} (4\sigma T_w^4 - G_w). \tag{22}$$

The absorption coefficients of the gas mixture ($\kappa$) is determined using a built-in gray gas model, whereas the wall has a constant value $\kappa_w$ of 0.6. Adding radiation to the problem alters the interface condition (Eq. (7)) to

$$\lambda_{eff} \frac{\partial T_f}{\partial y}\bigg|_{int,y=+0} + q_{r,in} - q_{r,out} = \lambda_s \frac{\partial T_s}{\partial y}\bigg|_{int,y=-0}, \tag{23}$$

where $q_{r,in}$ is the incident radiative heat flux absorbed by the solid and $q_{r,out}$ is the reflected and emitted radiative heat flux leaving the solid.

**Table 1** Boundary and initial conditions for Sandia Flame D. zG stands for the Neumann boundary condition zeroGradient. The axial-velocities are expressed in m/s, and the temperatures in K. Species are denoted in mass fractions

| Variable | Fuel jet | Pilot jet | Co-flow | Gas-wall interface | Outer wall surface | Side wall surfaces |
|---|---|---|---|---|---|---|
| $U_{\text{axial}}$ (m/s) | 49.6 | 11.4 | 0.9 | 0 | – | – |
| $T$ (K) | 294 | 1880 | 291 | Coupled | 291 | zG |
| $Y_{CH_4}$ | 0.1561 | 0 | 0 | zG | – | – |
| $Y_{O_2}$ | 0.1966 | 0.054 | 0.23 | zG | – | – |
| $Y_{N_2}$ | 0.6473 | 0.742 | 0.77 | zG | – | – |
| $Y_{H_2O}$ | 0 | 0.0942 | 0 | zG | – | – |
| $Y_{CO_2}$ | 0 | 0.1098 | 0 | zG | – | – |

# 3 Numerical Set-Up

## *3.1 Test Cases*

The solver is tested on two methane-air combustion cases. In the first case, the implementation of combustion in the new solver is validated with experimental data from a turbulent piloted diffusion flame from the Sandia National Laboratories (Sandia Flame D). The burner dimensions can be found here [4].

For the second case, CHT is incorporated and the Sandia Flame D is confined by a cylindrical wall made of refractory material, with inner and outer diameters of respectively 300 and 360 mm. The axial length of the calculation domain (excluding fuel and pilot channels) is 600 mm. The boundary conditions of the two cases can be found in Table 1. The wall has the following thermal properties: a density of $2800\,\text{kg}\,\text{m}^{-3}$, a thermal conductivity ($\lambda_s$) of $2.1\,\text{W}\,\text{m}^{-1}\,\text{K}^{-1}$, a specific heat capacity ($c_p$) of $860\,\text{J}\,\text{kg}^{-1}\,\text{K}^{-1}$ and a radiative emissivity ($\kappa_s$) of $0.6\,\text{m}^{-1}$.

The computational domains of cases 1 to 2 consist of respectively 38,000 and 43,000 quadrilateral cells.

# 4 Results and Discussion

## *4.1 Case 1*

In Fig. 1 the temperature along the axis of symmetry is plotted. It shows that the multiRegionReactingFoam's prediction is identical to that of reactingFoam, as would be expected when CHT is switched of. Both solvers over-predict the ignition delay, temperature rise and peak temperature with the 2-step reaction mechanism. When using the full GRI reaction mechanism, these features are better captured and show good agreement.

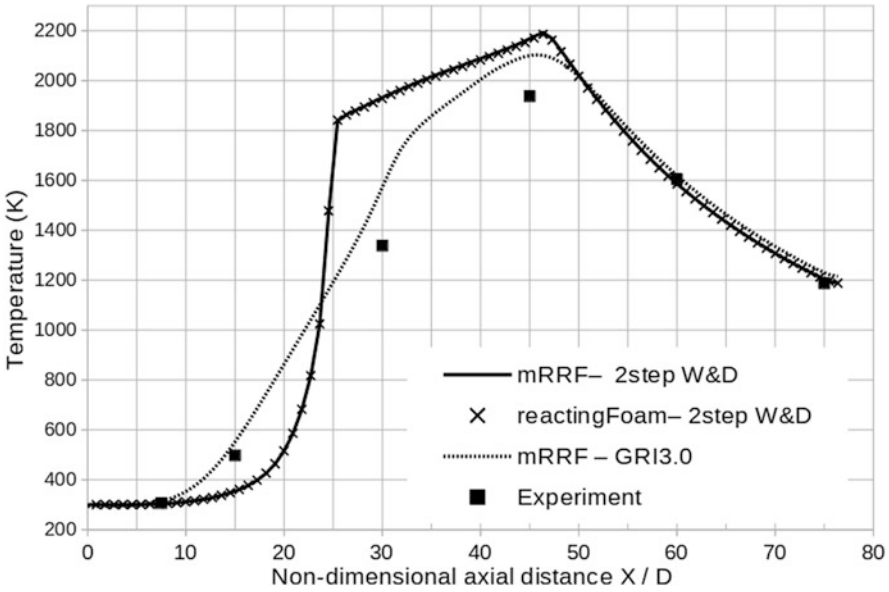


**Fig. 1** Temperature progression along the centre line (Case 1)

## *4.2 Case 2*

Now that a wall is introduced around the Sandia Flame D, it absorbs some of the energy, as can be seen in Fig. 2. Figure 3 shows a decomposition of the heat transfer to the wall in which the wall is being heated only due to thermal radiation. The wall is not heated via convection due to the fact that the hot gas heated by the flame leaves the domain before coming into contact with the wall. In fact, the convective heat transfer part plays a cooling role by transferring some of the wall's heat to the cold adjacent air, hence the negative contribution.


**Fig. 2** Contour plot of the temperature (Case 2)

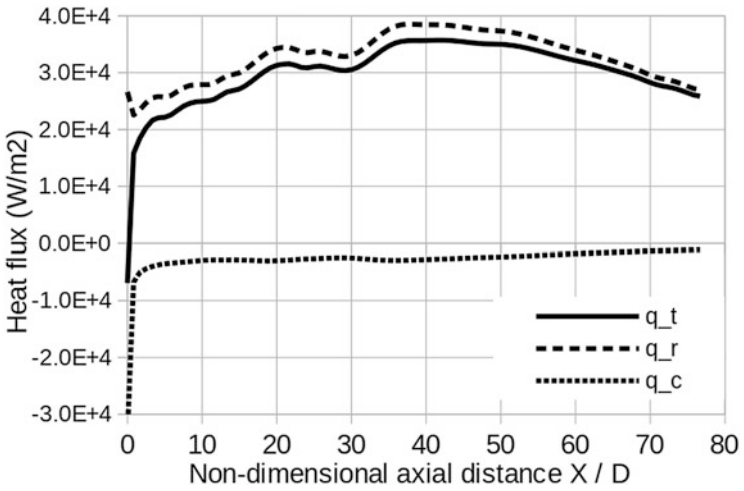


**Fig. 3** Heat flux along the inner wall surface (Case 2). q_t, q_r and q_c are respectively the total, radiative and convective heat fluxes

## 5 Conclusions

This work has shown that OpenFOAM's standard solvers reactingFoam and chtMultiRegionFoam are successfully implemented in the new solver multiRegionReactingFoam. This enables the modelling of combustion with conjugate heat transfer. The results of the new solver, with conjugate heat transfer turned off, are identical to reactingFoam and good agreement is shown with experiments when using the full GRI mechanism. Also the flame-wall interaction is shown when enabling conjugate heat transfer. This still requires to be validated.

**Acknowledgments** The authors would like to thank Eric Daymo from Tonkomo LLC for developing the solver multiRegionReactingFoam and for his collaboration on debugging the solver in order to make it more robust.

## References

1. Source code of chtMultiRegionReactingFoam. https://github.com/TonkomoLLC. Accessed: 2017-01-15.
2. E.A. Daymo and M. Hettel. Chemical reaction engineering with DUO and chtMultiRegionReactingFoam. 4th OpenFOAM User Conference 2016, Cologne-Germany, 2016.
3. T. Poinsot and D. Veynante. *Theoretical and Numerical Combustion*. R.T. Edwards, Inc., Philadelphia, 2nd edition, 2005.
4. Sandia flame D test description on the ERCOFTAC QNET-CFD wiki forums. http://qnet-ercoftac.cfms.org.uk/w/index.php/Description_AC2-09. Accessed: 2016-07-01.